

Riverine flood assessment in Jhang district in connection with ENSO and summer monsoon rainfall over Upper Indus Basin for 2010

Bushra Khalid^{1, 2, 3, 4}, Bueh Cholaw¹, Débora Souza Alvim⁵, Shumaila Javeed⁶, Junaid Aziz Khan⁷, Muhammad Asif Javed⁸, Azmat Hayat Khan⁹

Corresponding author's email: kh_bushra@yahoo.com

Corresponding author's mobile: 0092-3315719701

¹International Center for Climate and Environment Sciences,
Institute of Atmospheric Physics, Chinese Academy of Sciences, Beijing 100029, China

²Earth System Physics, *The Abdus Salam* International Centre for Theoretical Physics,
Trieste, Italy

³Department of Environmental Science, International Islamic University, Islamabad, Pakistan

⁴International Institute for Applied Systems Analysis, Laxenburg, Austria

⁵Center for Weather Forecasting and Climate Studies, National Institute for Space Research,
Cachoeira Paulista, São Paulo, Brazil

⁶Department of Mathematics, COMSATS Institute of Information Technology, Islamabad,
Pakistan

⁷Institute of Geographical Information System (IGIS), National University of Science and
Technology (NUST), Islamabad, Pakistan

⁸Department of Humanities, COMSATS Institute of Information Technology, Islamabad,
Pakistan

⁹Pakistan Meteorological Department, Quetta, Pakistan

1 **Abstract**

2
3 Pakistan has experienced severe floods over the past decades due to climate
4 variability. Among all the floods, the flood of 2010 was the worst in history.
5 This study focuses on the assessment of 1) riverine flooding in the district Jhang
6 (where Jhelum and Chenab rivers join, and the district was severely flood
7 affected) and 2) south Asiatic summer monsoon rainfall patterns and anomalies
8 considering the case of 2010 flood in Pakistan. The land use/cover change has
9 been analyzed by using Landsat TM 30 m resolution satellite imageries for
10 supervised classification, and three instances have been compared i.e., pre
11 flooding, flooding, and post flooding. The water flow accumulation, drainage
12 density and pattern, and river catchment areas have been calculated by using
13 Shuttle Radar Topography Mission digital elevation model 90 m resolution. The
14 standard deviation of south Asiatic summer monsoon rainfall patterns,
15 anomalies and normal (1979-2008) have been calculated for July, August, and
16 September by using data set of Era interim 0.75° resolution. El Niño Southern
17 Oscillation has also been considered for its role in prevailing rainfall anomalies
18 during the year 2010 over Upper Indus Basin region. Results show the
19 considerable changing of land cover during the three instances in the Jhang
20 district and water content in the rivers. Abnormal rainfall patterns over Upper
21 Indus Basin region prevailed during summer monsoon months in the year 2010
22 and 2011. The El Niño (2009-2010) and its rapid phase transition to La Niña
23 (2011-2012) may be the cause of severity and disturbances in rainfall patterns
24 during the year 2010. The Geographical Information System techniques and
25 model based simulated climate data sets have been used in this study which can
26 be helpful in developing a monitoring tool for flood management.

27
28 **Key words:** Flooding, riverine, ENSO, monsoon, rainfall, land cover
29
30
31

32 **Introduction**

33

34 Pakistan has frequently faced many meteorological disasters such as droughts
35 and floods due to climate variability. These disasters caused environmental
36 damages, fatalities, economic losses and displacement of population (Hashim et
37 al. 2012; Federal Flood Commission of Pakistan 2011; Khan & Khan 2015;
38 National Disaster Management Authority 2011). These natural hazards cannot
39 be prevented however the likelihood of human exposure to them can be
40 mitigated through proper planning and management strategies. El Niño
41 Southern Oscillation (ENSO) is the climate variability that causes fluctuations
42 in ocean temperatures over the equatorial Pacific. ENSO shows substantial
43 impacts on global climate and weather over the years (Hirons and Klingaman
44 2016). It has two phases, a warm phase, i.e., El Niño; when the ocean water
45 becomes substantially warmer than normal (Yu et al. 2017), and a cold phase
46 called La Niña; when the ocean water becomes substantially colder than normal
47 and is considered nearly reverse pattern to that of El Niño (Deflorio et al. 2013;
48 Goly and Teegavarapu 2014). ENSO has afflicted Pakistan with above or below
49 normal rainfalls in different periods during the past decades (Rashid 2004; Arif
50 et al. 2006; Mahmood et al. 2004; Khan 2004). Weather anomaly prevails over
51 Pakistan during ENSO and affects summer and winter rainfall (Rashid 2004;
52 Khan 2004). The summer monsoon rainfall faces deficit over Pakistan during El
53 Niño events and cause meteorological droughts (a condition that may occur
54 when precipitation is insufficient to meet the needs of established human
55 activities (Hoyt 1938)) (Rashid 2004), whereas it receives near-normal to
56 above-normal rainfall during La Niña years (Khan 2004), that usually cause
57 flooding. La Niña conditions often, though not always, follow the El Niño
58 conditions (Hirons and Klingaman 2016).

59 The abnormal weather conditions prevailed during summer monsoon season
60 over Pakistan in 2010; consequently, Pakistan received higher than normal and
61 spatially distributed rainfall which caused flooding in the Indus, Jhelum and
62 Chenab Rivers. The Indus River, with a length of 3,180 km and an average
63 annual discharge of 7610 m³/s, is the largest river of Pakistan and its major
64 tributaries are Jhelum and Chenab Rivers (Gaurav et al. 2011; Ahmad 1993).

65 The Jhelum River drains an area that lies in the west of Pir Panjal separating
66 Jammu and Kashmir and flow southward parallel to the Indus at an average
67 elevation of 1680 meters. About 6000 Km² of alluvial lands are drained in the
68 Kashmir valley by Jhelum River (Babel and Wahid 2008). It receives water
69 from several important sources such as glaciers located in the northern areas of
70 Pakistan (IUCN 2007). Based on a 20 years record at the rim stations of
71 Pakistan (inflow measurement facility has been established at the rim of the
72 Indus River tributaries and thus referred to as Rim station inflows), the main
73 contribution to the inflow comes from the rivers of Indus, Jhelum and Chenab,
74 which accounts for more than 95% of the total flow (Ahmad 1993; Ahmad
75 2000).

76 River Indus and its tributaries (Sutlej, Ravi, Jhelum and Chenab Rivers)
77 irrigates the vast plains on the south of Salt range extending to the Arabian Sea,
78 and east of Sulaiman and Kirthar mountain ranges. These tributaries meet the
79 Indus River at Mithan Kot. On the north of the Mithan Kot, there lies the Upper
80 Indus Basin (UIB) and on the south lies the Lower Indus Basin. The northern
81 areas of the Indus River are very fertile despite of the fact that this is an arid
82 region. The fertility in this region is mainly due to the soil brought by the
83 Rivers. The UIB consists of the northern areas of Pakistan extending to the
84 south up to Sargodha High (Iqbal 1995). UIB comprise of northern areas of
85 Pakistan i.e., mountain ranges including Himalayas, Hindu Kush, Pamirs, and
86 Karakoram (Ferguson 1985), provinces of Khyber Pakhtunkhwa, Punjab and

87 Jammu & Kashmir and are covered by Jhelum & Chenab Rivers (Babel and
88 Wahid 2008), in addition to the River Indus and its other small tributaries.

89 Pakistan is highly vulnerable to hydro-meteorological events and has
90 experienced recurring cycles of riverine flooding over the past several years.
91 The flooding in Pakistan during the summer monsoon months of July-
92 September 2010 was 7.5 on scale of intensity. The 2010 flood affected
93 approximately one-fifth of Pakistan's total land area and displaced 20,000,000
94 inhabitants with 2000 fatalities in the country (Brakenridge 2012; Chorynski et
95 al. 2012). Flooding in the Jhelum & Chenab Rivers started in late July and
96 sustained by the end of 2010 due to abnormally intensified summer monsoon
97 rainfall in UIB (Syvitski and Brakenridge 2013). Several studies have
98 investigated the effects of recent and of past riverine flooding in different parts
99 of Asian continent (as shown in Table. 1).

100 The present study investigates land use/cover assessment using supervised
101 classification mode during 2010 flooding of the Jhelum and Chenab Rivers in
102 the district Jhang, and monsoon rainfall patterns in UIB. Jhang district lies in the
103 Punjab province with an area of 8,809 Km² and an estimated population of
104 466,121 people (for 2010) (Punjab Development Statistics 2014). The two
105 rivers i.e., Jhelum and Chenab meet in Jhang district at the point called the
106 Trimmu Headworks (Fig. 1). The water flow in the Indus River, the past floods
107 in the Indus River, and the overall flood situation during 2010 in Pakistan have
108 been discussed in detail in several studies (e.g., Syvitski and Brakenridge 2013;
109 Hashmi et al. 2012; Mustafa & Wrathall 2011). General waterways along the
110 Indus River, general satellite imaging comparison of flood extent for monsoon
111 period in 2009 and 2010, and non-meteorological reasons of flooding over
112 Pakistan have been already discussed and published (e.g., Arslan et al. 2013;
113 Khan et al. 2014; Gaurav et al. 2011; Webster et al. 2011; Akhtar 2012; Syvitski
114 and Brakenridge 2013; Mustafa and Wrathall 2011). Hashmi et al. (2012)

115 conducted a comprehensive study on the capacity of different Pakistan's rivers
116 and barrages to explore their role in flood mitigation. However, the land
117 use/cover and changes during and after flooding in Jhelum & Chenab River
118 catchment areas have not been studied to provide useful information for policy
119 making and implementing mitigation plans for metropolitan areas. This study
120 provides an insight into the weather conditions of summer monsoon rainfall
121 prevailed during 2010 over UIB in comparison to the normal rainfall, rainfall
122 anomalies and ENSO. This study focuses on filling the afore knowledge gap
123 and aims at developing an understanding on the use of combined techniques in
124 Geographical Information System and reanalysis climate data as a monitoring
125 tool in flood management in future.

126 **Materials and Methods**

127 Shuttle Radar Topography Mission (SRTM) Digital Elevation Model (DEM) 90
128 meters resolution has been used for the calculation of water flow direction, flow
129 accumulation, drainage density and pattern, catchment areas, and stream feature
130 in Jhang district. Landsat TM imageries consisting seven spectral bands have
131 been downloaded from USGS website. 6 bands (i.e., bands 1 to 5 and 7) have a
132 spatial resolution of 30 meters whereas band 6 (thermal infrared) has a 120
133 meters resolution and is re-sampled to 30 meters. The imageries of May 2009,
134 August 2009 and July 2010 have been processed for 'pre-flooding', imageries
135 of August 2010 and September 2010 have been processed for 'flooding', and
136 imagery of December 2010 has been processed for the 'post flooding' instances.
137 The simulated data of rainfall (mm/day) of Era interim ($0.75^\circ \times 0.75^\circ$ resolution)
138 has been downloaded from European Centre for Medium-Range Weather
139 Forecasts (ECMFW) website for the years of 1979-2011. Data was analyzed for
140 30 years (i.e., 1979-2008) to calculate climatology (rainfall) for the summer
141 monsoon months i.e., July, August, and September (JAS); and average daily
142 rainfall, anomalies, and standard deviations for JAS for the years of 2009-2011.

143 Daily rainfall trend (mm/day) over UIB for 1979-2016 has been shown by using
144 Era interim (0.75° x 0.75° resolution) data set. The El Niño events from 1981-
145 2017 have been described by using daily Nino4 index from SST OI v2 ¼ degree
146 (K).

147 Digital satellite images have pixel values and need to be calibrated to convert
148 into reflectance. Calibrating imagery is a pre-processing step which removes
149 radiometric errors caused by sensor's scanning angle and distortion in an image
150 that produces noise in addition to the true spectral radiance. ENVI's Radiometric
151 Calibration tool provides options to calibrate imagery to radiance, reflectance,
152 or brightness temperatures. We calibrated all the images and changed them from
153 digital number (DN) values to reflectance. Radiometric Calibration tool also
154 helps in classification to understand the objects by checking their spectral
155 profile and reflectance in various bands.

156 Catchment delineation refers to the process of using DEM to identify features
157 such as streams, catchment areas, and basins etc. The first input required for
158 catchment delineation is DEM. DEM data files contain the elevation of the
159 terrain over a specified area, usually at a fixed grid interval over the "Bare
160 Earth". ArcGIS was used to delineate the smaller catchments in the study area.
161 A high flow accumulation shows the areas of concentrated flow which are down
162 slope or on the flat surface, and can be used to identify the channels of stream.
163 The zero flow accumulation areas represent the topographic highs. The drainage
164 pattern was calculated by the polyline feature that in turn identifies the stream
165 order and stream feature. The stream feature represents the linear network.
166 Density of the drainage is calculated by stream feature that represent the linear
167 network. This linear network is used to calculate the line density. The line
168 density calculates the magnitude per unit area from polyline features which lie
169 within the radius around the pixel. The search radius of calculating the linear
170 network and density is 100 meters. The unit is based on the linear unit of the

171 projection of the output spatial reference. The similar technique has been used
172 by Khalid and Ghaffar (2015) for calculating the drainage density and patterns,
173 flow accumulation and stream feature in different cities of Pakistan. River
174 catchments were calculated by using the 'Watershed' application. A watershed
175 is an upslope area that contributes flow of water to a common outlet as
176 concentrated drainage. A larger watershed may contain many smaller
177 watersheds, called sub-basins or catchments. In this study, calculation of river
178 catchments determines those areas from which the Chenab and Jhelum Rivers
179 receive water toward the drainage basin to the extent of the Jhang district.

180 Supervised image classification using maximum likelihood algorithm is used for
181 mapping several classes for pre flooding, post flooding and flooding instances
182 in study area. Image classification is a well-used and accepted technique for
183 quantifying land cover and land use at a location and across multi-temporal
184 phases (Alphan et al. 2009). Five classes have been identified i.e., water,
185 vegetation, built-up area, soil and clouds for the study area. Maximum
186 likelihood algorithm is the statistical decision in which the pixels are assigned to
187 the class of highest probability. This gives more accurate results as compared to
188 other algorithms. Some images of the year 2010 (August and September) had
189 cloud cover which cause difficulty in classification as areas under cloud cover
190 and cloud shadow reflect differently thus difficult to identify.

191 The classified imageries were compared to give a clear picture of the pre
192 flooding, post flooding and flooding time situation in Jhang district. The
193 climatic analysis has been performed to understand the anomaly and usual trend
194 of rainfall in the region considering 30 years as normal (i.e., 1979-2008) for
195 JAS. Furthermore, the rainfall trends in JAS for the years of 2009-2011 were
196 also mutually compared to see the variations during the flood season of year
197 2010. The standard deviation average anomaly for climatic normal (1979-2008)

198 and standard deviation anomaly for JAS (2009-2011) has been calculated to
199 observe the variations of rainfall over UIB.

200 **Results**

201 Flow direction determines the flow of water in any of the eight directions as
202 shown in Fig. 2. Flow accumulation conditions and drainage density of the
203 Jhang district are shown in Fig. 3. The streams show the areas of concentrated
204 flow and high drainage density. Total streams in the catchments identified in the
205 study area (8809 Km²) are 189 as shown in Fig. 4. Three instances of pre-
206 flooding, flooding and post-flooding were processed and compared to estimate
207 the change in land use/cover in the Jhang district along Jhelum and Chenab
208 Rivers.

209 The images of May 2009, August 2009 and July 2010 are classified for pre-
210 flooding instance. These images were compared to observe land use/cover
211 before flooding (Figs. 5-8). The change detection statistics shows no significant
212 change in built up area (Table 2), hence built up is represented as '0' in flooding
213 instance while vegetation, water and soil were changed about 39.02%, 30.10%
214 and 21.28% respectively. The image classification of August 2010 and
215 September 2010 shows the flooded district in Figs. 9 & 10. Vegetation cover in
216 August and September is about 54% and 55% respectively. Water covered
217 about 10% and 5% of area in August 2010 and September 2010 respectively.
218 Soil cover was classified about 15% and 17% in August and September 2010
219 respectively. An additional class was identified which affected the classification
220 i.e., cloud cover, typically found during monsoon season and has been
221 considered as a class which is about 8% and 7 % in August 2010 and September
222 2010 respectively as shown in Fig. 11. In the post flooding instance, vegetation
223 cover has identified as 29%, soil 25%, water 1% and built up area 44% (see

224 Figs. 12 & 13). The overall change in area covered by different identified
225 classes is shown in Table 3.

226 The climatic normal (1979-2008) have been analyzed for JAS in UIB (Fig. 14).
227 The analysis shows that the rainfall in July 2009 is less than normal (Fig. 15);
228 abnormally intense conditions (causing heavy rains) prevailed in July 2010 (Fig.
229 16); the rainfall pattern observed to be normal in July 2011 (Fig. 17). Normal
230 conditions are observed for August 2009 whereas abnormal conditions prevailed
231 during August 2010 and August 2011 (Figs. 16 & 17). Normal conditions are
232 observed in September 2009 and September 2011 whereas abnormal conditions
233 prevailed in September 2010 (Figs. 15-17). Figs. 18-20 illustrate the prevailing
234 anomaly during the year 2010 which can be seen when compared to the
235 situations of 2009 and 2011. During 2010, an intense anomaly occurred over
236 UIB during July and August. Figs. 21-22 show the standard deviations of
237 rainfall over UIB. Standard deviation of 2009-2011 has been compared with the
238 standard deviation of climatology (i.e., 1979-2008) (Fig. 21) that shows intense
239 occurrence of anomaly during July and August over UIB (Fig. 22). A surge in
240 rainfall events has been observed in years 1979, 1981, 1993, 1997, 2003, 2004,
241 2006, 2010, 2011, and 2016 (Fig. 23). The high values in years 1979, 2003,
242 2004 and 2006 is between two El Niño events whereas high values in 1981,
243 1993, 1997, 2010, 2011, and 2016 is between the events of El Niño and La Niña
244 (c.f. Fig. 24). The higher values show El Niño events and the lower values show
245 La Niña events (Fig. 24).

246 **Discussion**

247 SRTM DEM was acquired and preprocessed to determine flow direction, flow
248 accumulation, drainage density and to delineate the catchments of study area
249 and is shown in Figs. (2-4). The water flow is south and south-eastward,
250 catchments meet up in the south and drainage density becomes higher at this

251 point where Rivers of Jhelum and Chenab meets. The catchments with highest
252 water flow are dark blue whereas areas with the lowest flow are red. The high
253 flows are apparent in the areas where both the rivers of Jhelum and Chenab
254 merge. The catchments drain all the water to a single point and form a drainage
255 pattern (Fig. 4).

256 The pre-flooding, flooding, and post flooding instances have been discussed in
257 the following section. The land preparation and sowing season starts in April
258 and May for Kharif crops (the crops cultivated and harvested in South Asian
259 countries in summer monsoon season which bring rains that lasts from April to
260 October depending on the area) that is why most of the area in district Jhang has
261 been classified as soil/open land. The Punjab province starts to receive monsoon
262 rains by the end of June that helps in cultivation for Kharif crop. Therefore area
263 in May 2009 has been shown as covered with vegetation by around 26.1% of
264 the Jhang district and has further considered in vegetation class. This is also the
265 time when harvesting of sugarcane starts in this region. Vegetation cover has
266 increased in pre flooding instance i.e., August 2009 and in flooding instance in
267 July 2010 respectively as the cultivation of other crops like rice and maize etc.
268 increases at this time. No significant change has been observed in built up area
269 while water cover has significantly increased in August 2009 and July 2010 due
270 to summer monsoon rainfall and riverine flooding. Flood hit the Jhang district
271 in August 2010 and receded slowly. The classified imageries of August 2010
272 (Fig. 9) and September 2010 (Fig. 10) show the flooded district. The vegetation
273 is lush during August 2010 and September 2010 and increased chlorophyll
274 content has been recorded during these months which are identified in NIR
275 bands. August showing the highest vegetation covers in comparison to all
276 instances. In September 2010 vegetation cover decreases because of crops'
277 harvesting. Here it is observed that 5% of water receded in a span of one month.
278 Water class is increased in flooding instance to about 5 times as compared to the

279 pre-flooding instance. The soil cover decreased to about half of what it was in
280 pre-flooding instance. Most important impact of flood is observed on built up
281 area class that enormously reduced from 44% in August 2009 to 13% and 14%
282 in August 2010 and September 2010 respectively. Analysis of satellite
283 imageries for above mentioned period shows that most of the built up area was
284 affected during the flood. Post-flooding instance clearly depicts the flooded
285 water has almost completely receded and again the land preparation period for
286 new cultivation has been started. Vegetation is only 29% in the post flooding
287 instance as it is the harvesting and land preparation season. Built up area is
288 again recovered and identified in December 2010 imagery after the flood water
289 has receded. Built up area is about 44% as it was in pre-flooding instance.
290 Water has regained its position and covers the river course only which is about
291 2%. Soil is identified around 25% which is almost the same as it was in pre-
292 flooding instance. Comparison of pre and post flooding images with flooding
293 instance show the significant change in built up area. Built up area has increased
294 in post-flooding month probably due to receded water and rehabilitation
295 activities. Water content was highest in August 2010 due to flooding while it
296 slowly receded back in post flooding instance. Vegetation content is at its peak
297 in August and September of both years (2009 & 2010); chlorophyll content is
298 found largely in crops in these months and is identified in near Infrared bands.
299 In May 2009 and December 2010, vegetation is less and bare soil has shown an
300 increasing trend.

301 The floods of 2010 negatively affected the socio-economic activities and human
302 settlements all over Pakistan and in the Jhang district. The flooding caused due
303 to higher than normal summer monsoon rainfall in the UIB. The water flows
304 south and south eastward towards the human settlements and passes through the
305 provinces of Khyber Pakhtun Khawa (KPK), Punjab, and Sind before it meets
306 Arabian Sea in the south. Severe rainfall with abnormal trends during 2011

307 compared to previous years was also observed in the study area. According to
308 the National Disaster Management Authority (2011), approximately 6,006,545
309 people from 23 districts were affected and 14,187 people were injured due to
310 floods all over the country.

311 It is clear from climatic analysis Figs. 14-20 the intense rainfall pattern has been
312 shown in UIB during JAS 2010 and August 2011. The summer monsoon
313 rainfall had deviated pattern and intense anomalies prevailed in 2010. The
314 standard deviation charts also showing the change in rainfall patterns in 2009-
315 2011 as compared to the climatology standard deviation (Fig 21-22). The inter-
316 decadal climate variability has contributed to the exacerbation and severity of
317 floods in 2010 and 2011. ENSO Southern oscillation may have contributed to
318 the variability in summer monsoon rainfall during 2010. Pakistan receives less
319 than normal rainfall during El Niño years and the reverse effects have been
320 observed during La Niña years or between two El Niño events, and between
321 consecutive El Niño or La Niña events as shown by Figs 23-24. These figures
322 show abnormally intensified rainfall events as the El Niño dissipates or some
323 times between two El Niño events or between two consecutive El Niño and La
324 Niña events. The higher than normal rainfall in monsoon season of year 2010
325 may also be a similar effect of dissipating the El Niño of 2009-2010 or between
326 two consecutive events of El Niño (i.e., 2009-2010) and La Niña (i.e., 2011-
327 2012) following the pattern from the past. The warm pool El Niño of 2009-2010
328 is unique as it followed the strongest warming signal in the central Pacific but
329 rapidly decayed to strong La Niña of 2011-2012 (Kim et al. 2011). This El Niño
330 was not only the warm pool event with highest central Pacific sea surface
331 temperature anomaly but also the fastest phase transition to La Niña among
332 other warm pool El Niño events (Lee and McPhaden 2010; Kim et al. 2011).

333

334 **Conclusion**

335 This study focused on the land use/ cover changes occurred in the district Jhang
336 in Punjab province where the two large rivers i.e., Jhelum and Chenab Rivers
337 meets at the Trimmu Headworks. The Landsat TM satellite imageries have been
338 processed for supervised classification and five classes are identified i.e., water,
339 vegetation, built-up area, soil and clouds. The comparison of pre flooding,
340 flooding and post flooding instances revealed land cover changes during the
341 three periods in the Jhang district. Comparison of pre & post flooding instances
342 showed the significant decrease in built up area during flooding instances i.e.,
343 from 44% to 13%. Built-up area again increased in post flooding instance as the
344 water receded and post flooding re-habilitation activities. Water content is
345 maximum in the rivers in August 2010. Vegetation has shown a peak in August-
346 September 2009 and 2010 while in May 2009 and December 2010, vegetation
347 has decreased and bare soil has increased. River catchments, flow direction,
348 flow accumulation, drainage density and pattern have also been identified in the
349 study area using SRTM digital elevation model. The south Asiatic monsoon
350 pattern over UIB has also been analysed. The abnormal rainfall patterns
351 (anomalies) have been observed during 2010 and 2011 when compared to the
352 normal. The ENSO has been identified playing its role in disturbances generated
353 in summer monsoon rainfall patterns during 2010-2011. The abnormally
354 intensified El Niño during 2009-2010 and its rapid phase transition to La Niña
355 2011-2012 has contributed to the exacerbation and severity of rainfall over
356 Pakistan during 2010. An interactive automated application can be made on the
357 methodology which can serve the purpose of web-based flood delineation tool
358 involving GIS and reanalysis model data sets. Identified sub-basins can be
359 further used for flood risk mapping. This analysis can be used in further
360 management and planning for natural resource and flood management.

361

362 **Author's contributions**

363 BK and JAK designed research and maintained the pattern; DSA performed
364 climatic analysis; JAK, performed the remote sensing analysis; BK interpreted
365 the results of climatic & remote sensing analysis and prepared the manuscript;
366 SJ and MAJ contributed with expert guidance on technical aspects; BC
367 supervised and gave permission to conduct the research; MAJ and AHK revised
368 and improved the manuscript.

369 **Declaration of Competing Interests**

370 There are no competing interests among author and coauthors.

371 **References**

- 372
- 373 1. Arnell NW, Gosling SN (2016). The impacts of climate change on river
374 flood risk at the global scale. *Climatic Change*, 134: 387.
- 375 2. Arslan M, Tauseef M, Gull M, Baqir M, Ahmad I, Ashraf U, Tawabini
376 BS (2013). Unusual rainfall shift during monsoon period of 2010 in
377 Pakistan: Flash flooding in Northern Pakistan and riverine flooding in
378 Southern Pakistan. *African journal of environmental science and
379 technology*, 7: 882-890.
- 380 3. Akhtar S (2012). *South Asiatic monsoon and flood hazards in the Indus
381 River basin: a study of flood hazards in Pakistan paperback – August 7,
382 2012*. LAP LAMBERT Academic Publishing.
- 383 4. Alphan H, Doygun H, Unlukaplan YI (2009). Post-classification
384 comparison of land cover using multitemporal Landsat and ASTER
385 imagery: the case of Kahramanmaraş, Turkey. *Environmental monitoring
386 and assessment*, 151, 327-336.
- 387 5. Ahmad N (1993). *Water resources of Pakistan*. Publisher Shahzad Nazir,
388 Gulberg, Lahore, Pakistan

- 389 6. Ahmad S, Mohammad A, Khan ST (2000) Water resources of Pakistan-A
390 country report. Water Resources Research Institute, National Agricultural
391 Research Centre, Islamabad
- 392 7. Brakenridge GR (2012). Global active archive of large flood events:
393 Dartmouth Flood Observatory, University of Colorado.
- 394 8. Babel M, Wahid S (2008). Freshwater under threat: South Asia:
395 Vulnerability Assessment of Freshwater Resources to Environmental
396 Change. Nairobi, Kenya: United Nations Environment Programme.
- 397 9. Chohan K, Ahmad SR, Islam Z, Adrees M (2015). Riverine flood
398 damage assessment of cultivated lands along Chenab River using GIS
399 and remotely sensed data: A case study of district Hafizabad, Punjab,
400 Pakistan. Journal of geographical information system, 7: 506–526.
- 401 10. Chorynski A, Pinskiwar I, Kron W, Brakenridge R, Kundzewicz ZW
402 (2012). Catalogue of large floods in Europe in the 20th century, *in*
403 Kundzewicz, Z.W., ed., Changes in Flood Risk in Europe: Wallingford,
404 UK, IAHS Press Special Publication 10: 27–54.
- 405 11. Dewan TH (2015). Societal impacts and vulnerability to floods in
406 Bangladesh and Nepal. Weather and Climate Extremes, 7: 36-42.
- 407 12. Doocy S, Daniels A, Murray S, Kirsch TD (2013). The Human Impact of
408 Floods: a Historical Review of Events 1980-2009 and Systematic
409 Literature Review. PLOS Currents Disasters. doi:
410 0.1371/currents.dis.f4deb457904936b07c09daa98ee8171a.
- 411 13. DeFlorio MJ, Pierce DW, Cayan DR, Miller AJ (2013). Western U.S.
412 extreme precipitation events and their relation to ENSO and PDO in
413 CCSM4, J. Clim., 26, 4231–4243.
- 414 14. FFC (2011). Federal Flood Commission of Pakistan, Annual Flood
415 Report-2010.

- 416 15.Ferguson RI (1985). Runoff from Glacierized Mountains: A Model for
417 Annual Variation and Its Forecasting. *Water Resources Research* 21(5):
418 702–08.
- 419 16.Ghosh S, Mistri B (2015). Geographic Concerns on Flood Climate and
420 Flood Hydrology in Monsoon-Dominated Damodar River Basin, Eastern
421 India. *Geography Journal*, Article ID 486740. doi:10.1155/2015/486740.
- 422 17.Goly A, Teegavarapu RSV (2014). Individual and coupled influences of
423 AMO ENSO on regional precipitation characteristics and extremes,
424 *Water Resour. Res.*, 50, 4686–4709, doi:10.1002/2013WR014540.
- 425 18.Gaurav K, Sinha R, Panda PK (2011). The Indus flood of 2010 in
426 Pakistan: a perspective analysis using remote sensing data. *Nat Hazards*,
427 59: 1815-1826.
- 428 19.Hirons L, Klingaman N (2016). La Nina 2016/2017 historical impact
429 analysis. Report by Climate, environment, infrastructure and Livelihoods
430 Professional Evidence and Applied Knowledge Services (CEIL PEAKS)
431 programme, Evidence on Demand organization.
- 432 20.Hashmi HN, Siddiqui QTM, Ghumman AR, Kamal MA, Mughal HR
433 (2012). A critical analysis of 2010 floods in Pakistan. *African Journal of*
434 *Agricultural Research*, 7:1054-1067.
- 435 21.Hoyt, JC (1938). Drought of 1936, with discussion of the significance of
436 drought in relation to climate. U.S. Geological Survey, Water Supply
437 Paper No. 820. p. 1.
- 438 22.Iqbal B (1995). Petroleum geology of Pakistan. Pakistan Petroleum
439 Limited. Karachi, Pakistan.
- 440 23.IUCN (2007). Pakistan Water Gateway. Accessed online in June 2017 at
441 <http://www.waterinfo.net.pk/index.cfm>
- 442 24.Khalid B, Ghaffar A (2015). Dengue transmission based on urban
443 environmental gradients in different cities of Pakistan. *International*
444 *Journal of Biometeorology* 59: 267-283.

- 445 25.Khan AN, Khan SN (2015). Drought Risk and Reduction Approaches
446 in Pakistan. In: Rahman AU., Khan A., Shaw R. (eds) Disaster Risk
447 Reduction Approaches in Pakistan. Disaster Risk Reduction (Methods,
448 Approaches and Practices). Springer, Tokyo
- 449 26.Khan SI, Hong Y, Gourley JJ, Khattak MU, Groeve TD (2014). Multi-
450 Sensor Imaging and Space-Ground Cross-Validation for 2010 Flood
451 along Indus River, Pakistan. *Remote Sens*, 6: 2393-2407.
- 452 27.Kundzewicz ZW, Kanae S, Seneviratne SI, Handmer J, Nicholls N,
453 Peduzzi P, Mechler R, Bouwer LM, Arnell N, Mach K, Muir-Wood R,
454 Brakenridge GR, Kron W, Benito G, Honda Y, Takahashi K,
455 Sherstyukov B (2013). Flood risk and climate change: global and regional
456 perspectives. *Hydrological Sciences Journal*, 59(1): 1-28.
- 457 28.Khan AH (2004). The influence of La-Nina phenomena on Pakistan's
458 precipitation. *Pakistan Journal of Meteorology*, 1: 23-31.
- 459 29.Kim WM, Yeh SW, Kim JH, Kug JS, Kwon MH (2011).
460 The unique 2009–2010 El Niño event: A fast phase transition of warm
461 pool El Niño to La Niña. *Geophysical Research Letters*, 38: L15809.
- 462 30.Lee T, McPhaden MJ (2010). Increasing intensity of El Niño in the
463 central-equatorial Pacific, *Geophysical Research Letters*, 37: L14603.
- 464 31.Mahmood A, Masood AKT, Faisal N (2006). Relationship between El
465 Niño and summer monsoon rainfall over Pakistan. *Pakistan Journal of
466 Marine Sciences*, 15(2): 161-178.
- 467 32.Mahmood A, Masood AKT, Faisal N (2004). Correlation between
468 multivariate ENSO index (MEI) and Pakistan's summer rainfall. *Pakistan
469 Journal of Meteorology*, 1(2): 53.
- 470 33.Mustafa D, Wrathall D (2011). Indus Basin Floods of 2010: Souring of a
471 Faustian Bargain? Were the 2010 Pakistan floods predictable? *Water
472 Alternatives*, 4: 72-85.

- 473 34.National Disaster Management Authority (2011). NDMA annual report.
474 Islamabad, Pakistan.
- 475 35.Punjab Development Statistics (2014). Bureau of Statistics Punjab
476 Report. Pakistan.
- 477 36.Pal I, Singh S, Walia A (2013). Flood Management in Assam, INDIA: A
478 review of Brahmaputra Floods. International Journal of Scientific and
479 Research Publications, 3(10).
- 480 37.Rashid A (2004). Impact of El-Nino on summer monsoon rainfall of
481 Pakistan. Pakistan Journal of Meteorology, 35: 35-43.
- 482 38.Syvitski JPM, Brakenridge GR (2013). Causation and Avoidance of
483 Catastrophic Flooding along the Indus River, Pakistan. GSA Today,
484 23:4–10.
- 485 39.Tripathi P (2015). Flood Disaster in India: An Analysis of trend and
486 Preparedness. Interdisciplinary Journal of Contemporary Research, 2(4).
- 487 40.Torti J (2012). Floods in Southeast Asia: A health priority. Journal of
488 Global Health, 2(2): 020304.
- 489 41.UN Escape (2015). Disasters in Asia and the Pacific: 2015 year in review.
490 United Nations report. Economic and social commission for Asia and the
491 Pacific.
- 492 42.Webster PJ, Toma VE, Kim HM (2011). Were the 2010 Pakistan floods
493 predictable? Geophysical Research Letters, 38: L04806.
- 494 43.WWF (2001). Dams accused of role in flooding: Research Paper: "Dams
495 and Floods". World Wide Fund For Nature.
- 496 44.Yu L, Zhong S, Heilman WE, Bian X (2017). A comparison of the effects
497 of El Niño and El Niño Modoki on subdaily extreme precipitation
498 occurrences across the contiguous United States, J. Geophys. Res.
499 Atmos., 122, doi:10.1002/2017JD026683.

501 Tables

502

503 Table 1. Studies on riverine flooding in different parts of Asian continent

504

Sr.	Authors	Year of Publication	Regions of study for riverine flooding	
1	Arnell & Gosling	2016	Asia	505 506 507
2	Dewan	2015	Bangladesh & Nepal	508
3	Kundzewicz et al.	2013	Global	509
4	Doocy et al.	2013	Asia	510
5	Torti	2012	South Asia	511
6	WWF	2001	Southeast Asia	512
7	UN Escape	2015	Asia	513
8	Tripathi	2015	India	514
9	Pal et al.	2013	India	515
10	Ghosh and Mistri	2015	India	516
11	Chohan et al.	2015	Pakistan	517 518

519

520

521

522 Table 2: Change Detection Statistics for May 2009, August 2009 and July 2010

523

	Built Up	Water	Soil	Vegetation	Class Total
Water	0	69.897	5.003	5.398	100
Vegetation	0	12.12	11.242	60.976	100
Soil	0	9.248	78.718	29.487	100
Built Up	0	5.294	4.657	3.584	100
Class Total	0	100	100	100	0
Class Changes	0	30.103	21.282	39.024	0
Image Difference	0	188.269	25.865	-31.281	0

524

525

526

527

528

529

530

531

532

533

534

535

536

537

538

539

540

541

542

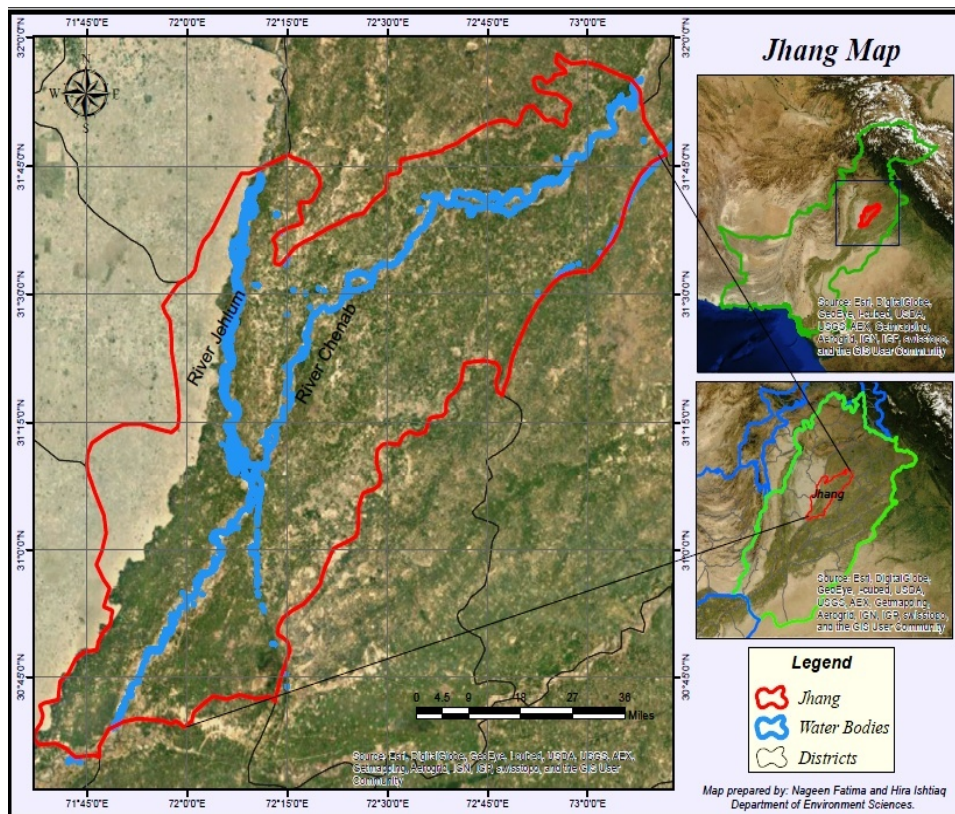
543

544 Table 3: Comparison of all classified images for change in covered area by different classes in Km²
 545

Class Names	May 2009	August 2009	July 2010	August 2010	September 2010	December 2010
Vegetation	2326.65	3634.54	3581.53	4789.99	4906.46	2611.84
Soil	2320.20	1038.04	1018.48	1338.35	1532.89	2221.83
Water	172.60	211.12	349.40	873.48	467.61	126.70
Built Up	4064.37	3991.5	3934.41	1162.71	1322.66	3923.45
Cloud	0.00	0	0.00	719.29	654.17	0.00
Total	8809.23	8809.54	8809.43	8809.35	8809.8	8809.46

546

547

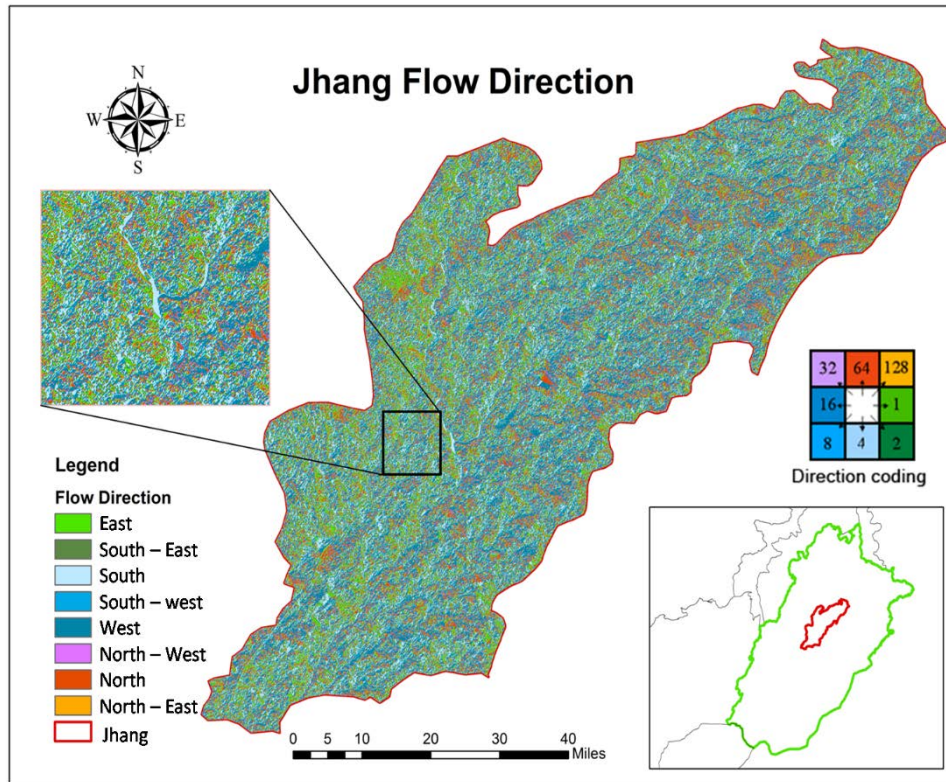


548

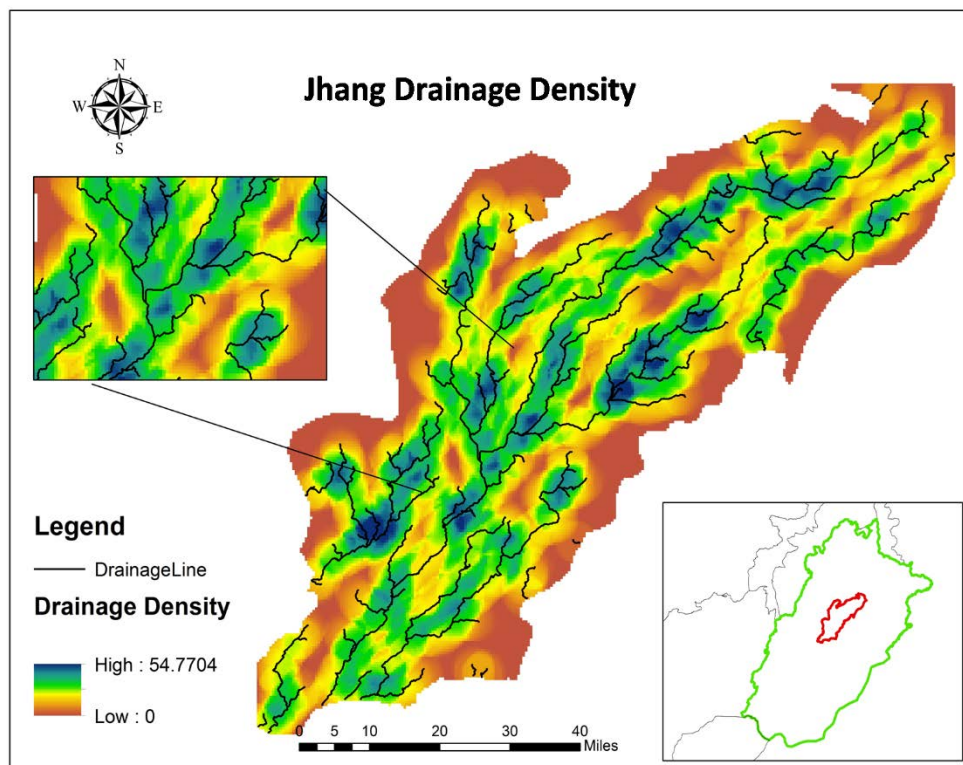
549

550 Fig 1. Map of study area showing the meeting point of Jhelum and Chenab Rivers on the
 551 boundary map of Jhang district; it is also showing the location of the Jhang district on the
 552 boundary map of Pakistan and on the boundary map of the Punjab province

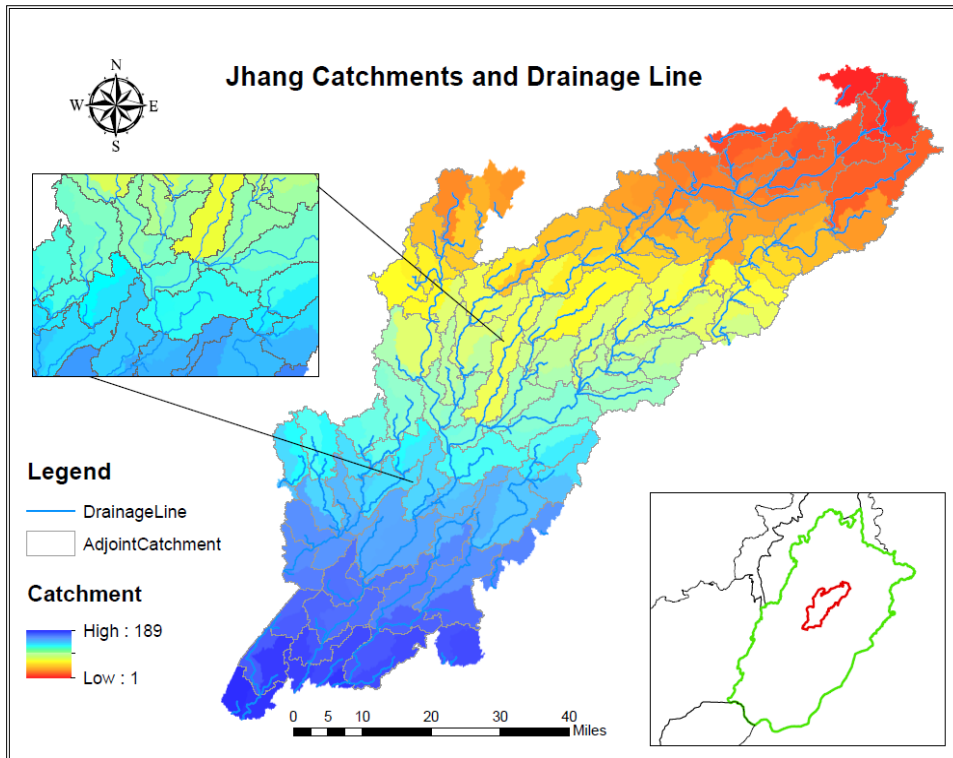
553



554
 555 Fig 2. Flow direction in the Jhang district has been shown, the water flow is mainly towards
 556 south and south east
 557



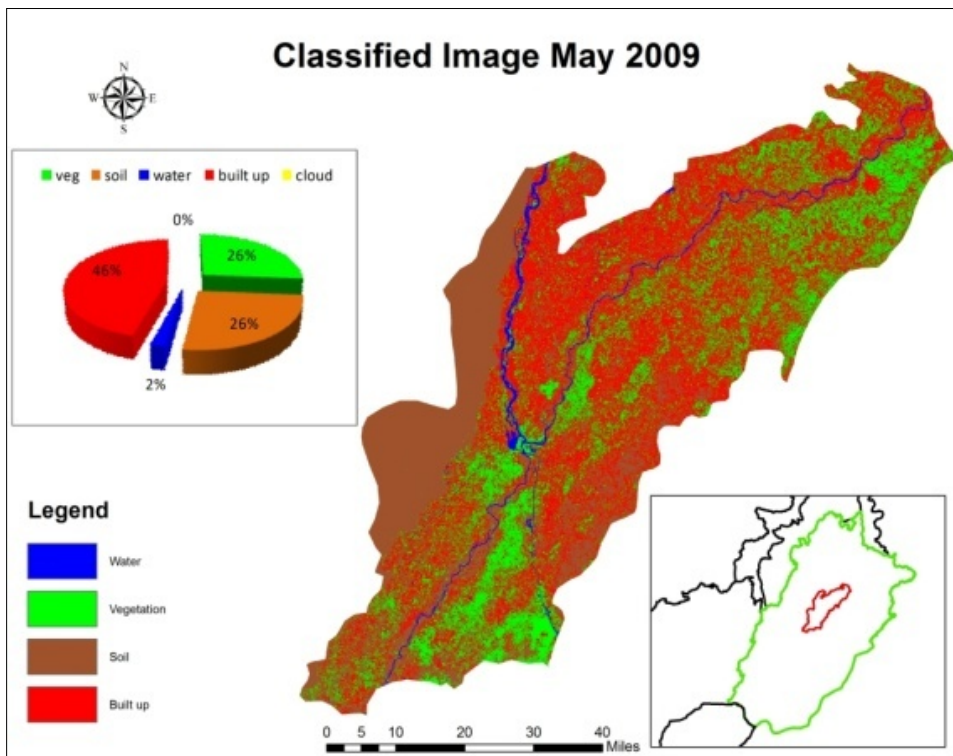
558
 559 Fig 3. High flow accumulation conditions represented by stream features and drainage
 560 density in different colors is shown in the Jhang district
 561



562
563
564
565
566
567
568
569

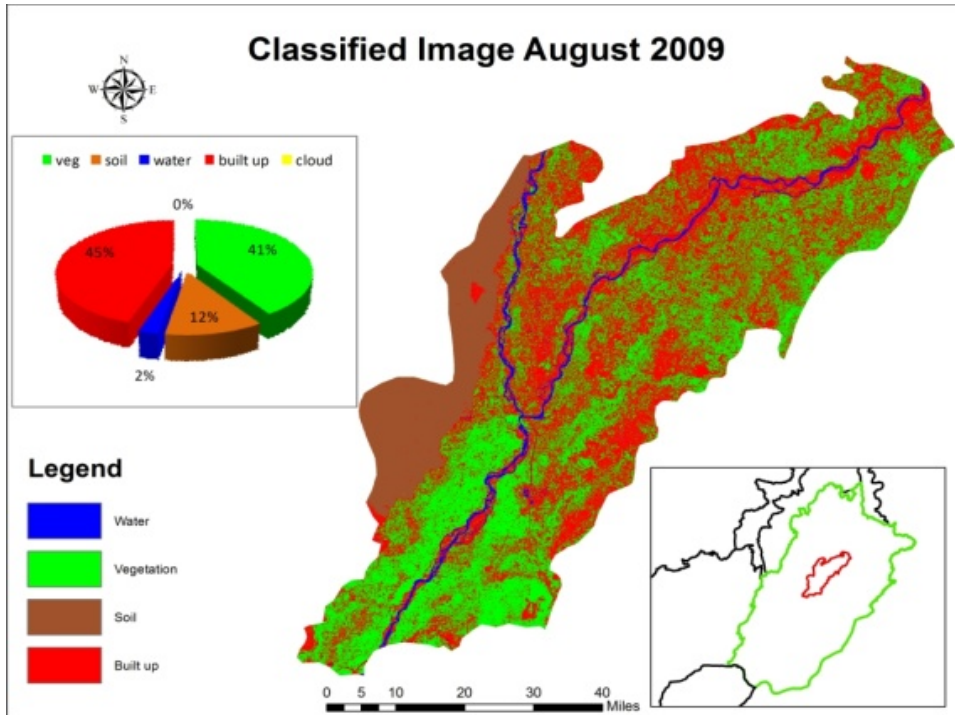
Fig 4. Identification of catchments in the Jhang district

1- Pre- Flooding instance



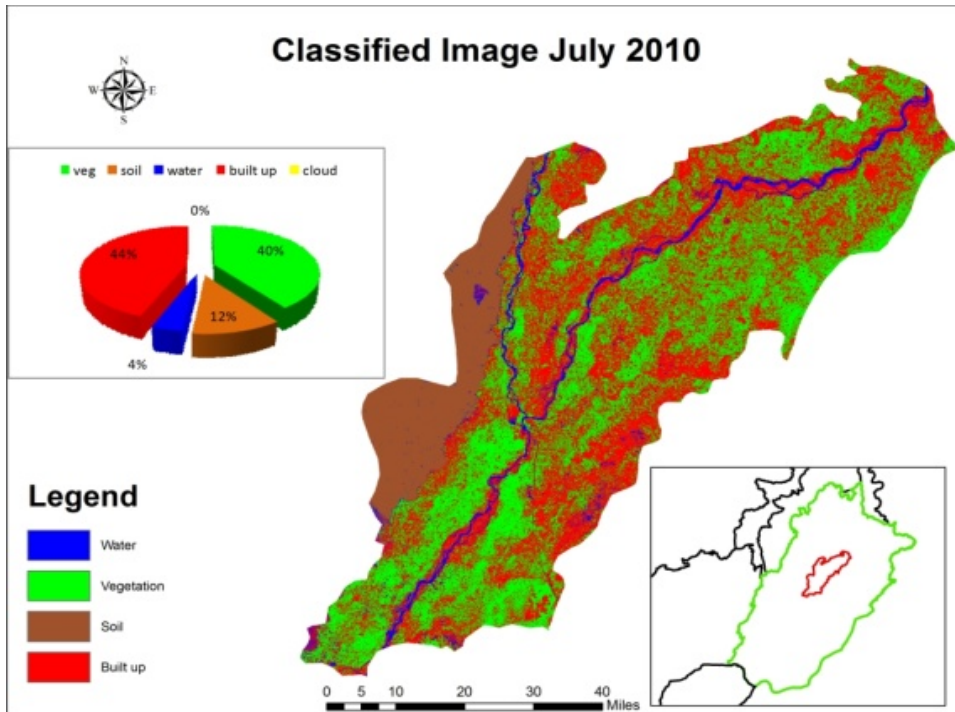
570
571
572

Fig 5. Classification of the Jhang district for May 2009 as pre flooding instance



573
574
575

Fig 6. Classification of the Jhang district for August 2009 as pre flooding instance



576
577
578

Fig 7. Classification of the Jhang district for July 2010 as pre flooding instance

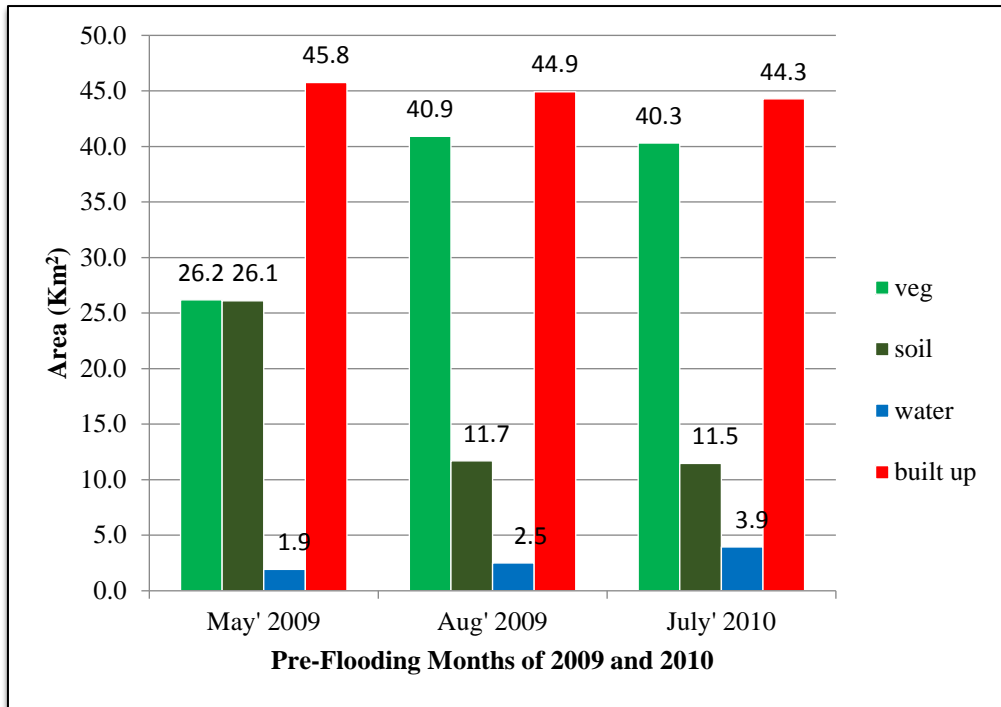
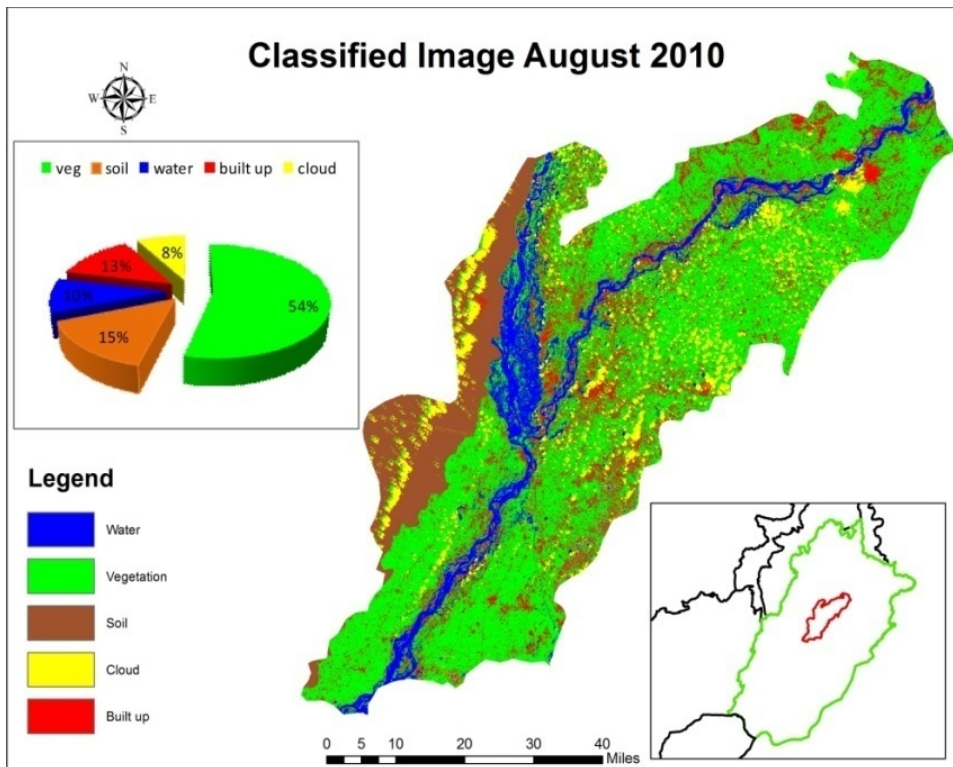


Fig 8. Comparison of results in pre flooding instance classification in the Jhang district for 2009-2010

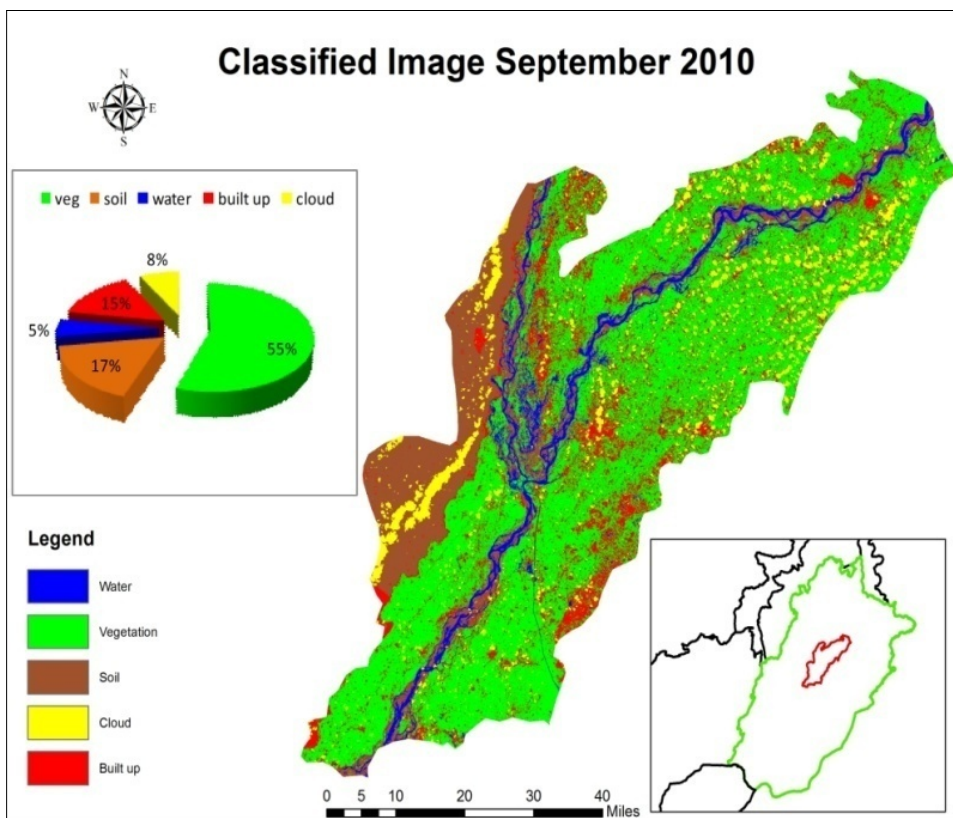
579
 580
 581
 582
 583
 584
 585
 586
 587
 588
 589
 590
 591
 592

2- Flooding instance



593
594
595

Fig 9 Classification of the Jhang district for August 2010 as a flooding instance



596
597
598

Fig 10 Classification of the Jhang district for September 2010 as a flooding instance

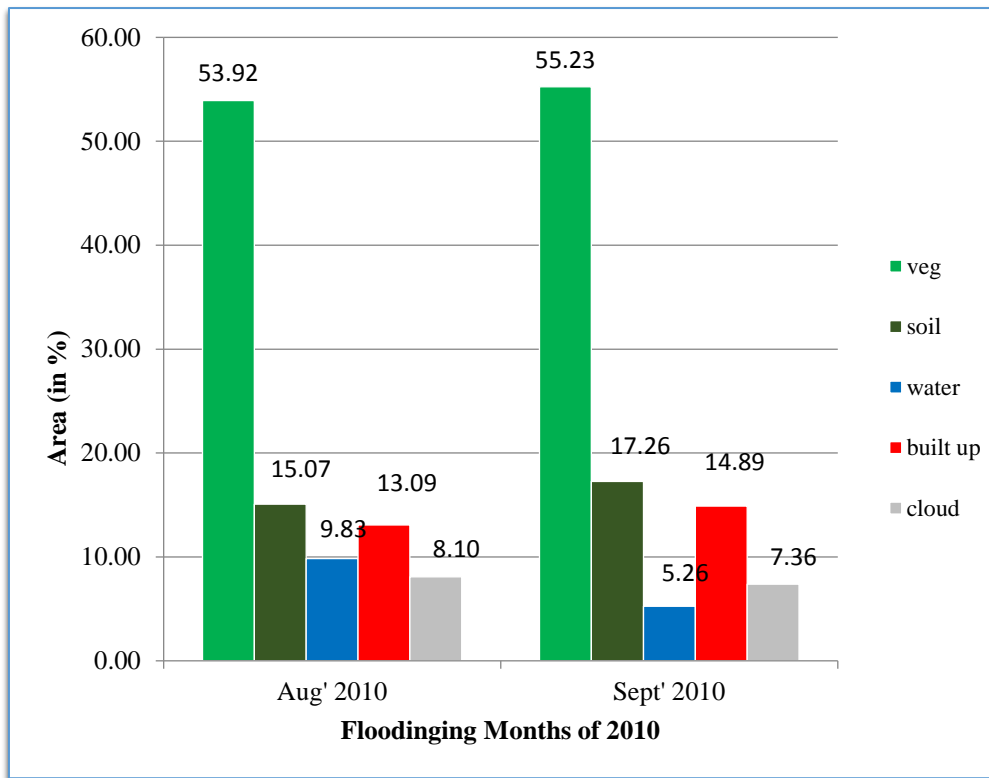


Fig 11. Comparison of identified classes in flooding classification instance in the Jhang district for year 2010

3- Post Flooding instance

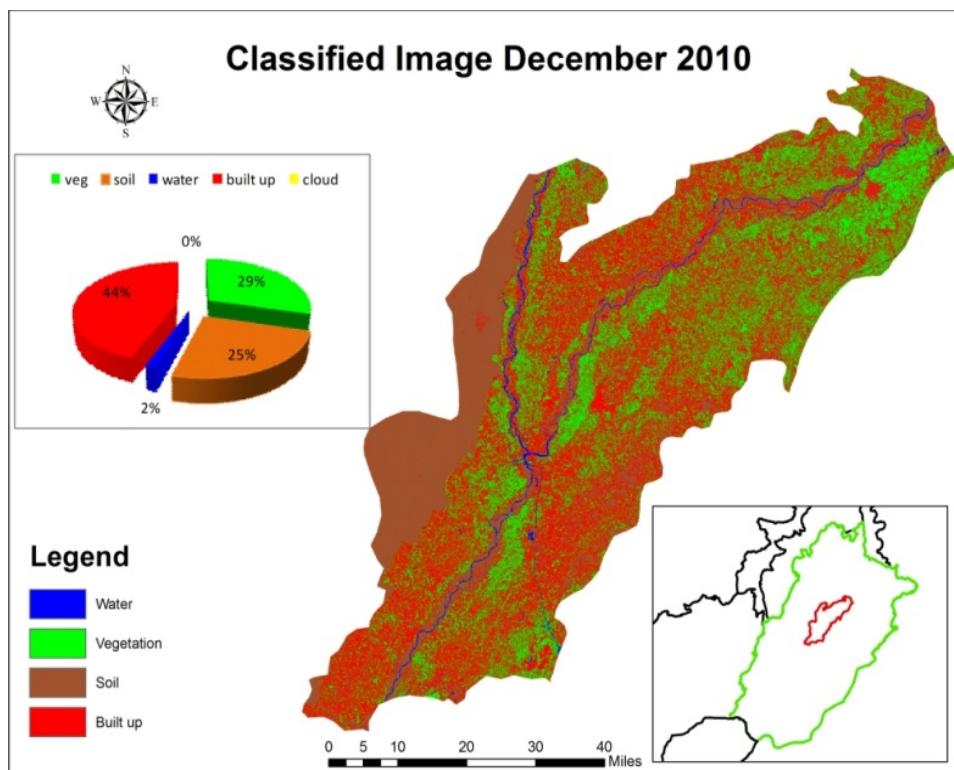
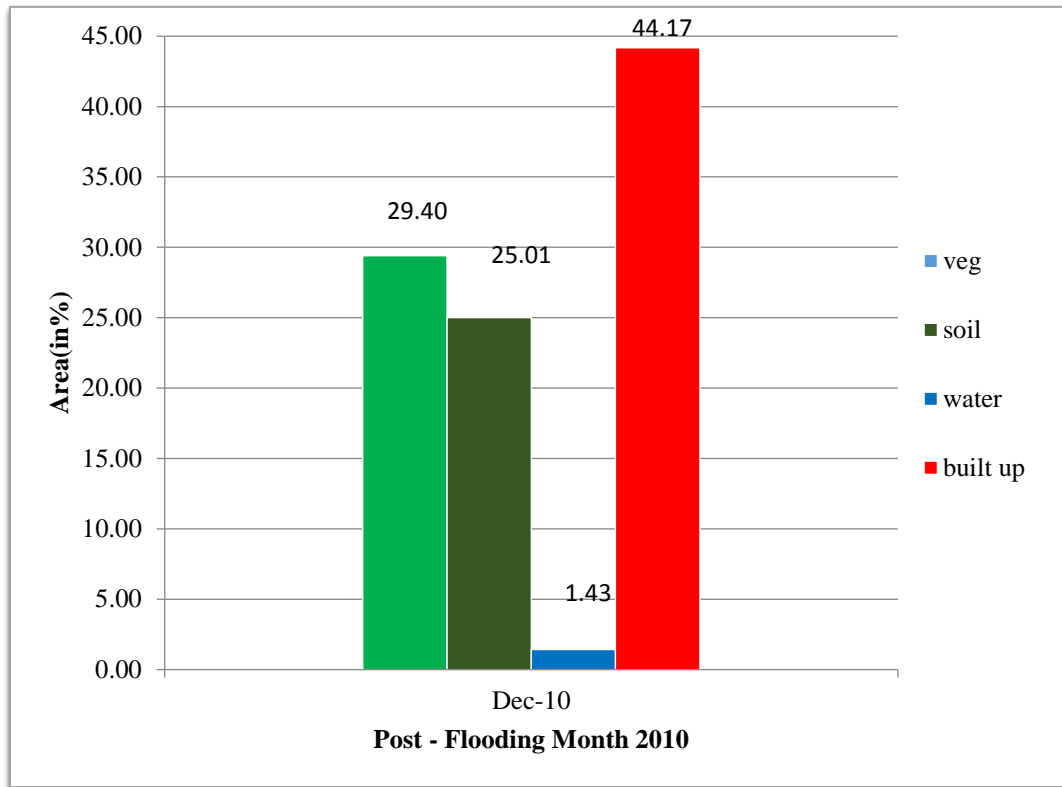


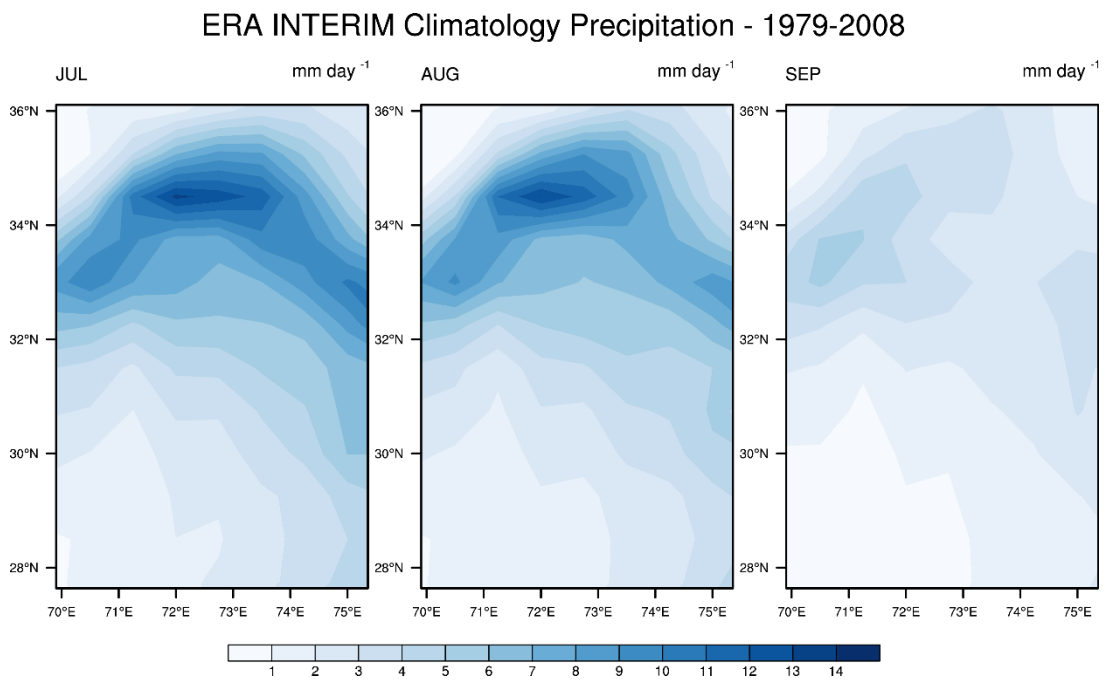
Fig 12 Classification of the Jhang district for December 2010 as a post-flooding instance

609



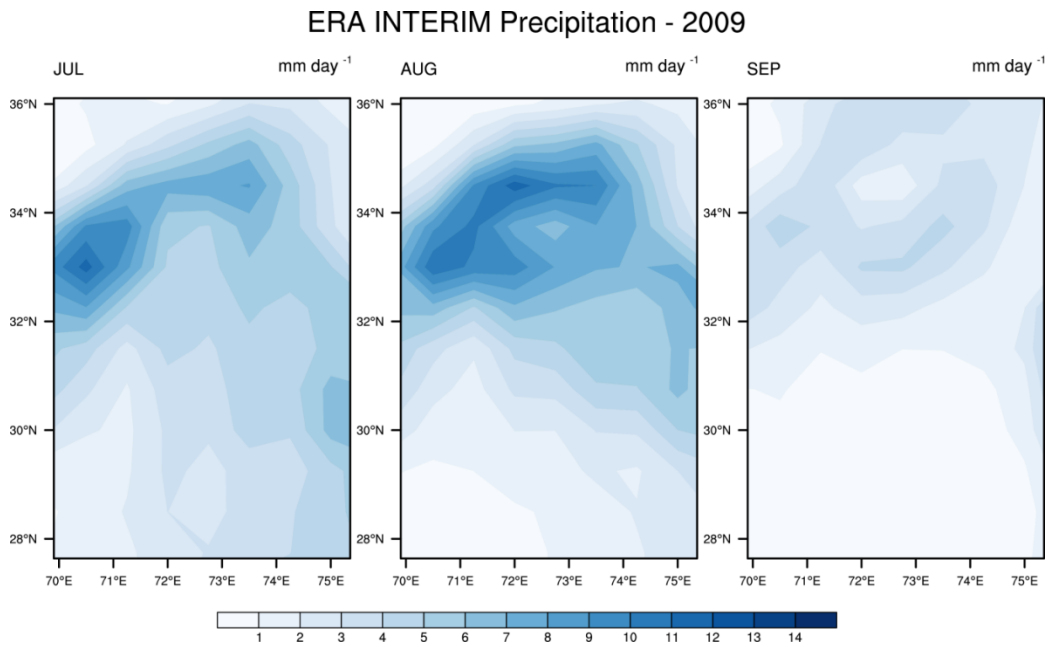
610
611
612
613

Fig 13. Comparison of identified classes in post-flooding classification instance in the Jhang district for year 2010



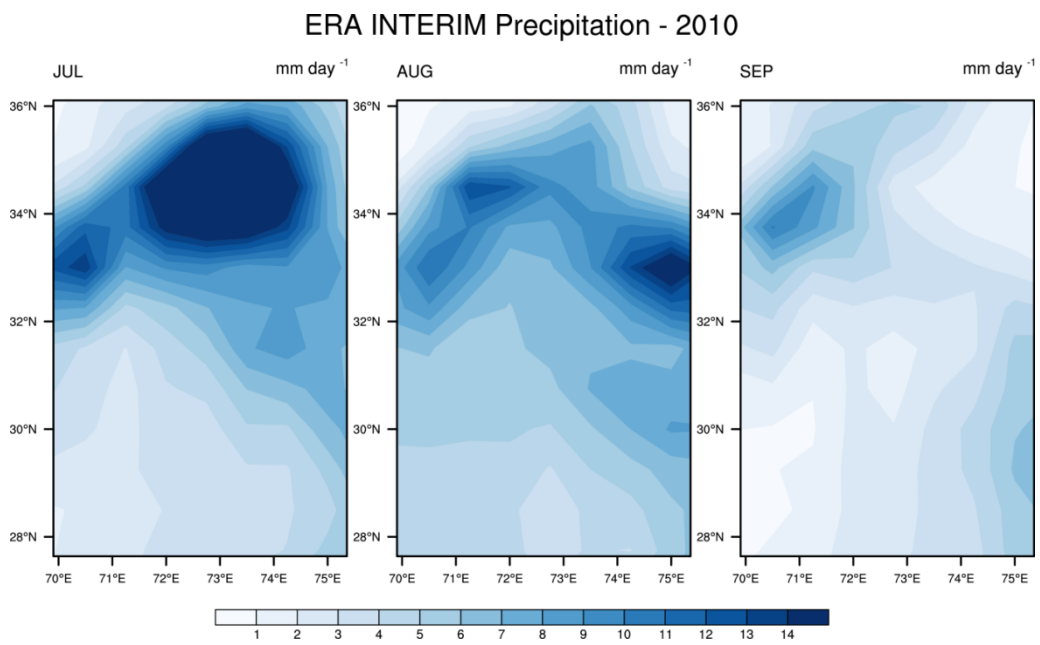
614
615
616

Fig 14. Climatology (1979-2008) showing rainfall patterns for JAS over UIB



617
618
619
620

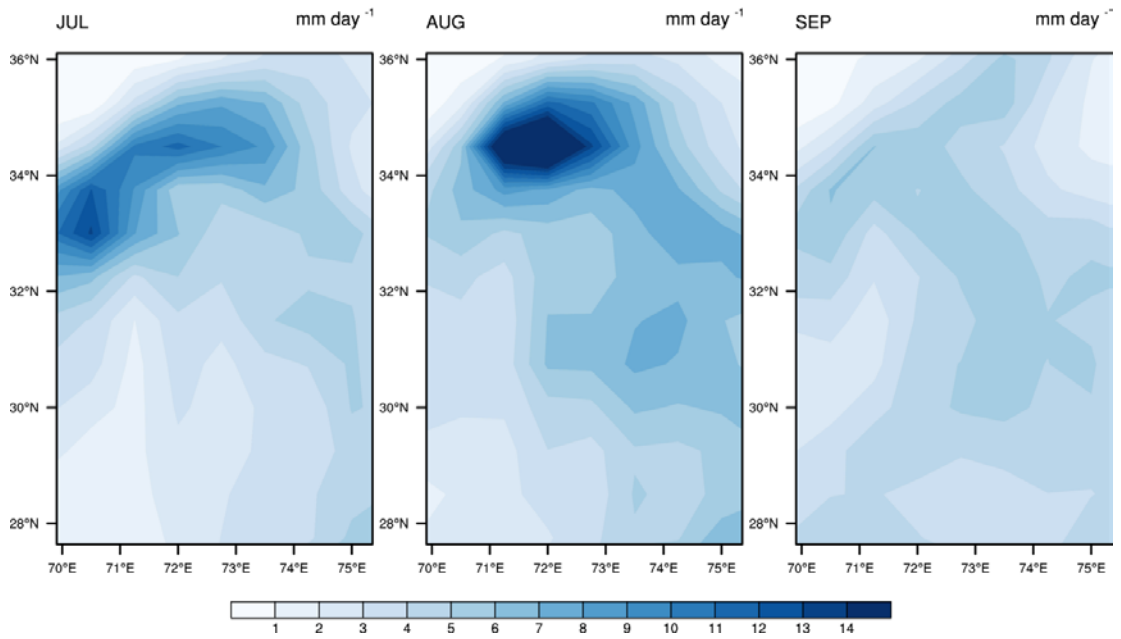
Fig 15. Rainfall pattern prevailed during 2009 over UIB in JAS



621
622
623

Fig 16. Rainfall pattern prevailed during 2010 over UIB in JAS

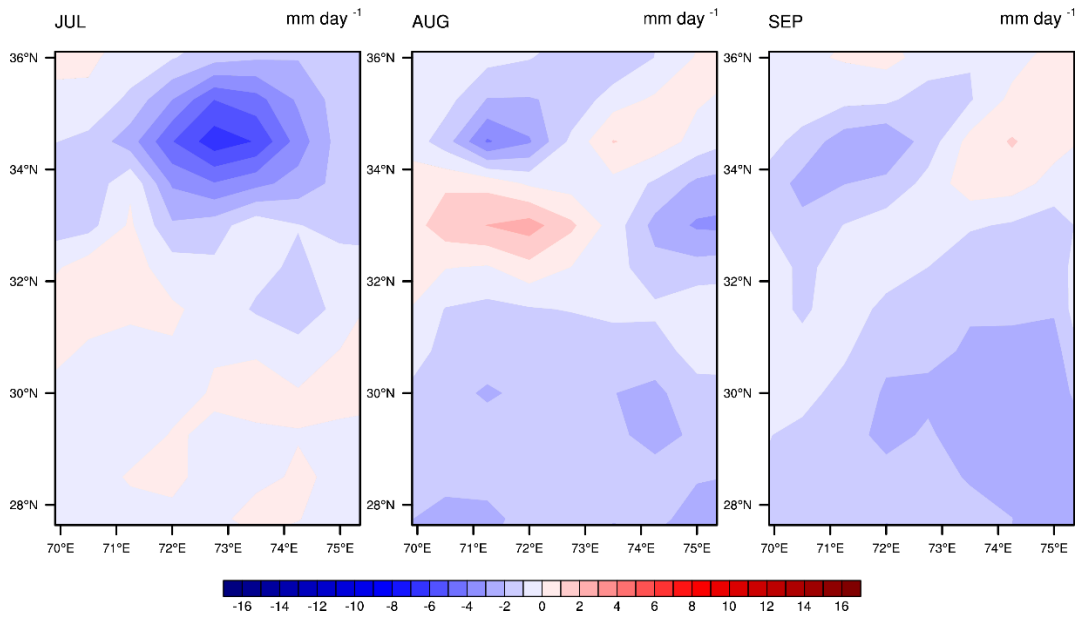
ERA INTERIM Precipitation - 2011



624
625
626
627

Fig 17. Rainfall pattern prevailed during 2011 over UIB in JAS

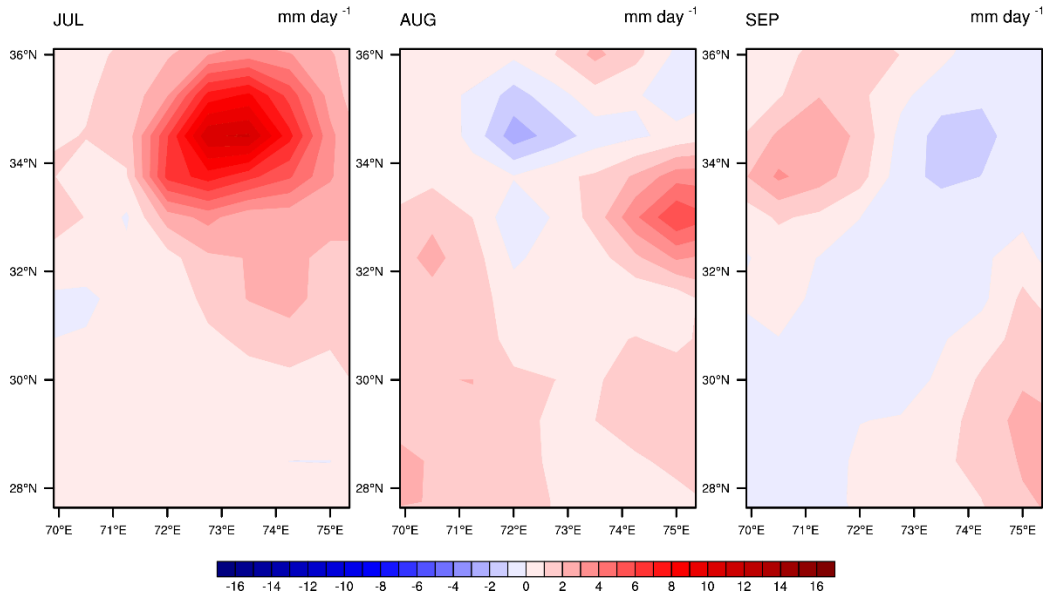
ERA INTERIM Anomaly Precipitation - 2009



628
629
630
631
632

Fig 18. Rainfall anomaly over UIB in JAS during 2009

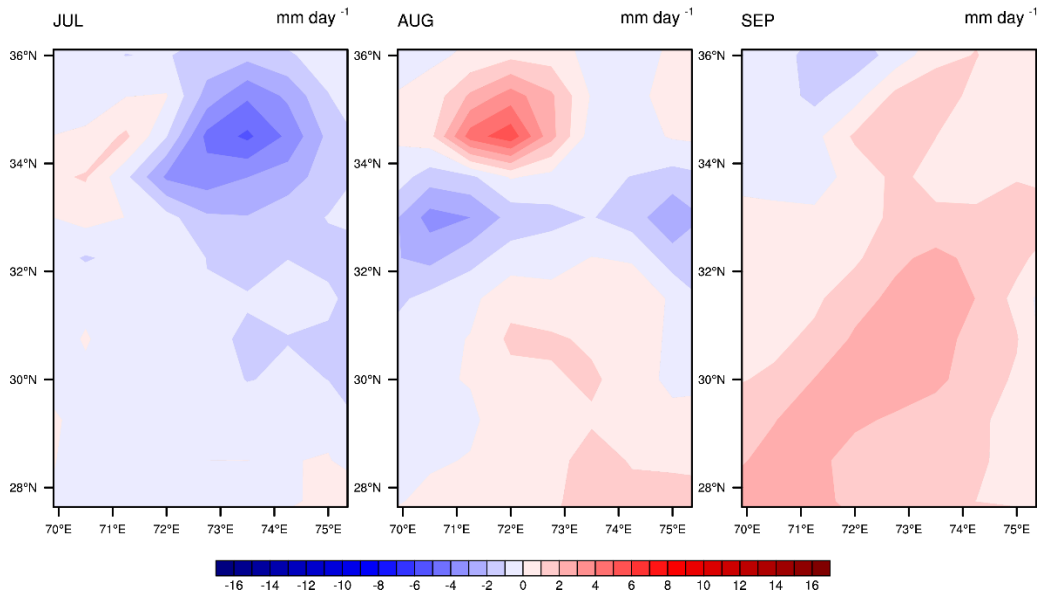
ERA INTERIM Anomaly Precipitation - 2010



633
634
635
636

Fig 19. Rainfall anomaly over UIB in JAS during 2010

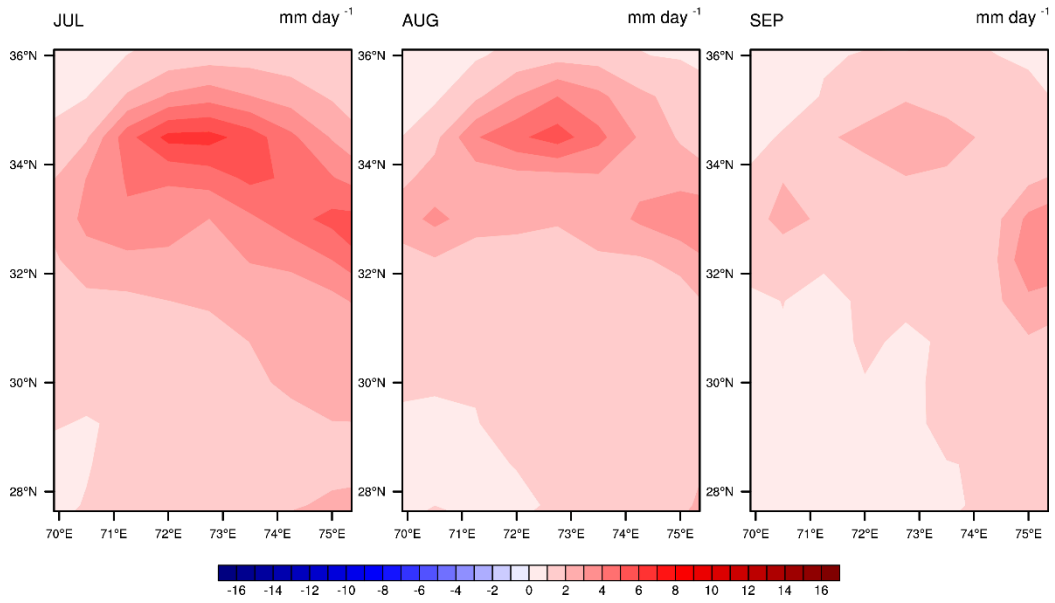
ERA INTERIM Anomaly Precipitation - 2011



637
638
639
640
641
642
643
644

Fig 20. Rainfall anomaly over UIB in JAS during 2011

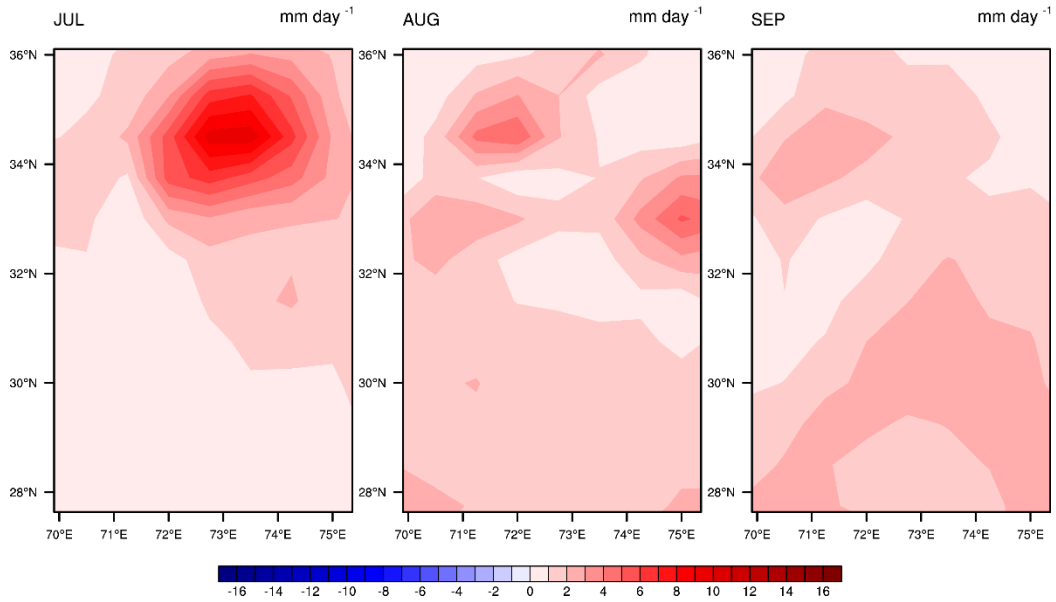
Standard deviation Climatology - 1979-2008



645
646
647
648
649

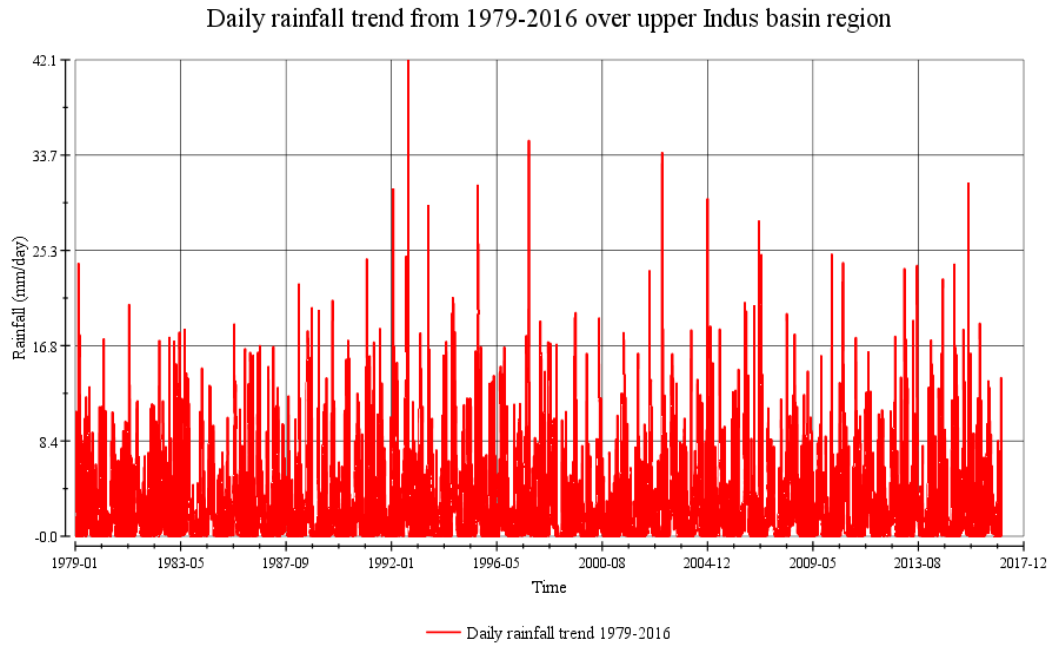
Fig 21. Standard deviation of climatology (1979-2008) over UIB during JAS

Standard deviation Climatology - 2009-2011



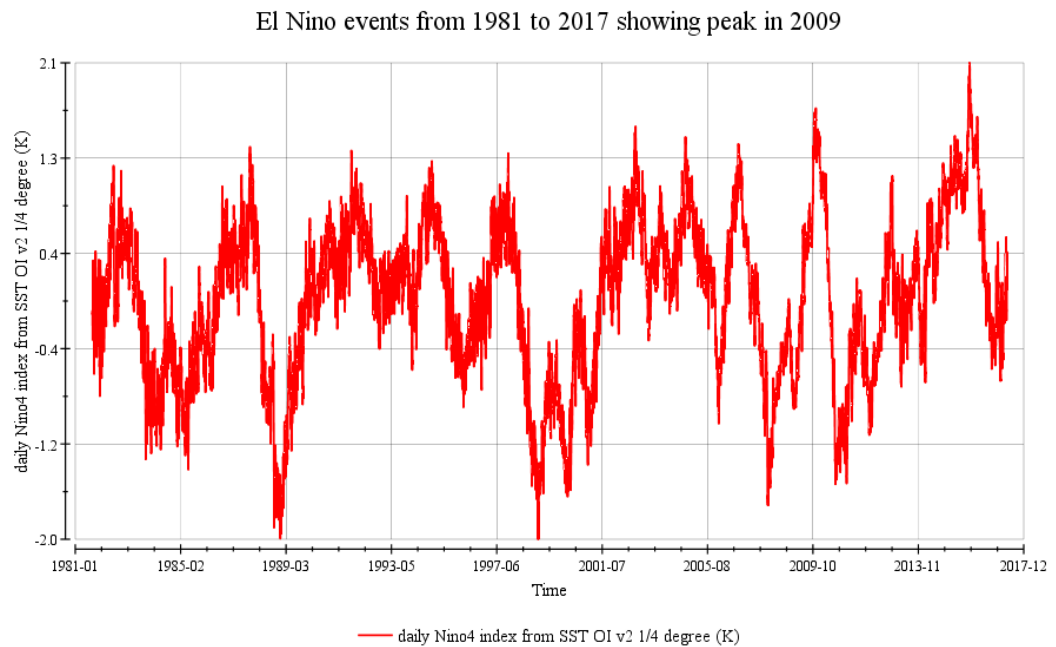
650
651
652
653
654
655

Fig 22. Standard deviation of climatology (2009-2011) over UIB during JAS



656
657
658

Figure 23. Rainfall trend in Upper Indus Basin region for 1979-2016



659
660
661
662
663

Fig 24. The peaks represents occurrence of El Nino while the lower values represents occurrence of La Nina events during 1981-2017